AD-A179 661 CONDITIONAL SECOND ORDER CLOSURE FOR TURBULENT SHEAR FLOWS(U) CALIFORNIA UNIV DAVIS DEPT OF MECHANICAL ENGINEERING W KOLLMANN 27 JUL 86 AFOSR-TR-87-0428 1/1

UNCLASSIFIED AFOSR-84-0219 F/G 20/4 NL

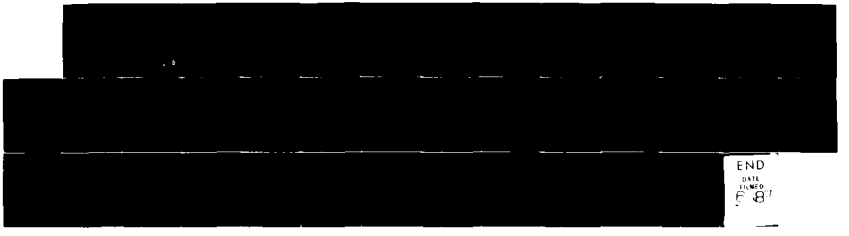

END

DATE FILMED

F 87

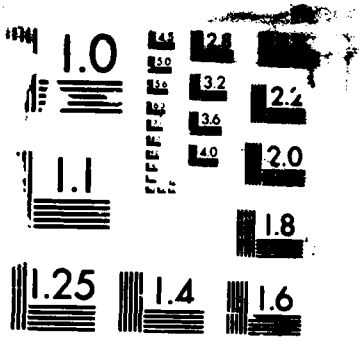
1.0
1.1
1.25
1.4
1.6
1.8
2.0
2.2
2.8
3.2
3.6
4.0
4.5
5.0

AD-A179 661

REPORT DOCUMENTATION PAGE

1a. REPORT SECURITY CLASSIFICATION: Unclassified	1b. RESTRICTIVE MARKINGS: None
2a. SECURITY CLASSIFICATION AUTHORITY	3. DISTRIBUTION / AVAILABILITY OF REPORT: Unlimited
2b. DECLASSIFICATION / DOWNGRADING SCHEDULE	
4. PERFORMING ORGANIZATION REPORT NUMBER(S): .	5. MONITORING ORGANIZATION REPORT NUMBER(S): AFOSR-TR- 87-0428
6a. NAME OF PERFORMING ORGANIZATION: University of California; 6b. OFFICE SYMBOL (If applicable): UCD	7a. NAME OF MONITORING ORGANIZATION: Air Force Office of Scientific Research
6c. ADDRESS (City, State, and ZIP Code): Dept. Mechanical Engineering, Davis, CA 95616	7b. ADDRESS (City, State, and ZIP Code): Bolling AFB, DC 20332-6448 BLDG 410
8a. NAME OF FUNDING / SPONSORING ORGANIZATION: Air Force Ofc. of Sci. Research; 8b. OFFICE SYMBOL (If applicable): AFOSR/NA	9. PROCUREMENT INSTRUMENT IDENTIFICATION NUMBER: AFOSR-84-0219
8c. ADDRESS (City, State, and ZIP Code): BLDG 410 Bolling AFB, DC 20332-6448	10. SOURCE OF FUNDING NUMBERS: PROGRAM ELEMENT NO. 61102F; PROJECT NO. 2307; TASK NO. A2; WORK UNIT ACCESSION NO.

11. TITLE (Include Security Classification): Conditional Second Order Closure for Turbulent Shear Flows

12. PERSONAL AUTHOR(S): Kollmann, Wolfgang

13a. TYPE OF REPORT	13b. TIME COVERED	14. DATE OF REPORT (Year, Month, Day)	15. PAGE COUNT
~~Scientific~~ ANNUAL	FROM 7.1.85 TO 6.30.86	1986.7.27	27

16. SUPPLEMENTARY NOTATION

17. COSATI CODES			18. SUBJECT TERMS (Continue on reverse if necessary and identify by block number)
FIELD	GROUP	SUB-GROUP	Turbulence, Closure, Shear Flow

19. ABSTRACT (Continue on reverse if necessary and identify by block number)

The properties of scalar variables, that allow to distinguish between turbulent and nonturbulent zones of shear flows, are investigated. The dynamics of the probability density function (pdf) of such a scalar is considered and a numerical solution technique based on stochastic simulation is developed. The second order closure is extended to axisymmetric shear flows and different closures for the turbulent transport of Reynolds stresses are evaluated.

20. DISTRIBUTION / AVAILABILITY OF ABSTRACT: ☒ UNCLASSIFIED/UNLIMITED ☐ SAME AS RPT. ☐ DTIC USERS	21. ABSTRACT SECURITY CLASSIFICATION: Unclassified
22a. NAME OF RESPONSIBLE INDIVIDUAL: J. McMichael	22b. TELEPHONE (Include Area Code): 202-767-4935; 22c. OFFICE SYMBOL: AFOSR/NA

DD FORM 1473, 84 MAR — 83 APR edition may be used until exhausted. All other editions are obsolete.

SECURITY CLASSIFICATION OF THIS PAGE

UNCLASSIFIED

CONDITIONAL SECOND ORDER CLOSURE FOR TURBULENT SHEAR FLOWS

W. Kollmann
Department of Mechanical Engineering, UCD
Davis, CA 95616

Annual Technical Report for Grant AFOSR-84-0219
1985/86

Attn: J. M. McMichael
AFOSR/NA
Bolling AFB
Washington, DC 20332

Annual report 1985/86

Grant: AFOSR-84-0219

Title: Conditional Second Order Closure For Turbulent Shear Flows

Prinipal Investigator W. Kollmann, UC Davis

Summary

The research work during the second year was concentrated on two subjects:

(1) Probability density functions and their application to conditional moment closures.

(2) Further development of the second order closure model based on conditional moments.

The work in the first area was concentrated on conditional closures treated on a higher level in terms of probability density functions. Since conditioning involves scalar variables such as enstrophy or small excess temperature scalar transport and stochastic techniques for the simulation in homogeneous and non-homogeneous turbulent flows were investigated (see Appendix I).

The work in the second area continued the effort of the first year and concentrated on axisymmetric flows. The differential equations constituting the closure model were transformed to cylindrical coordinates. The properties of different closure models for the turbulent transport of Reynolds stresses were evaluated first in the context of an unconditional second order closure (see Appendix II).

Research Objectives

The objective of the proposed research project is the development of a second order closure model for conditional moments and the intermittency factor. The foundation of the closure scheme are to be investigated and the resulting model should be applicable to a wide range of turbulent shear flows with free boundaries.

Status of Research

The research work on this project started in July 1984 with M. Mortazavi a Ph.D. student and S. Byggstoyl from TU Trondheim (Norway) as Postdoctoral fellow. The results from the first year were presented in the annual report for 1984/85. Byggstoyl has returned to Norway and A. Wu has joined as second Ph.D. student.

M. Mortazavi continued in the second year his work on the probability density formulation of conditional closures. He considered the turbulent transport of scalar variables such as temperature on enstrophy (vorticity squared), which can be used for discrimination between turbulent and non-turbulent zones in shear flows with a free boundary. The transport of scalar quantities in homogeneous turbulence was studied in terms of random walk simulations [4], and the main body of results is summarized in Appendix I. His results show that the stochastic simulation of two-point pdf's is very tedious. We decided therefore to concentrate on single-point pdf's. Currently work on the velocity-vorticity pdf equation is under way.

W. Kollmann spent eight months (August 85 to March 86) on sabbatical leave at the University of Zaragoza in Spain and collaborated with C. Dopazo on a research project related to the present contract. He devoted his research effort to the formulation of vorticity and enstrophy dynamics

in turbulent flows on the functional level where the resulting equations are exact and linear. It became clear during this period that the limit of infinite Reynolds-number plays a central role in the development of conditional closure schemes. The following time at UC Davis was devoted to the conditional second-order closure. The results obtained in the first year for plane flows [2],[3] showed that Lumley's [1] model for the turbulent transport of Reynolds stresses is advantageous. Hence we transformed the differential equations constituting the closure model to cylindrical coordinates. In order to evaluate the properties of several models for turbulent diffusion of stresses and dissipation rate a first test with the unconditional version of the second order closure was carried out. The results are presented in Appendix II, where the Daly-Harlow model (basically a gradient-flux model for turbulent stress transport) and Lumley's model are compared.

Arthur Wu joined the research effort at the beginning of the second year. He devoted his time to the development of a stochastic simulation technique for the solution of the velocity pdf-equations for developing (i.e. not necessarily self-similar) boundary-layer-type flows. This part was concluded successfully.

References

[1] J. L. Lumley, Advances in Appl. Mech. 18 (1978), pp. 123.

[2] S. Byggstoyl, W. Kollmann, Phys. Fluids 29 (1986), pp. 1423.

[3] S. Byggstoyl, W. Kollmann, Phys. Fluids 29 (1986), pp. 1430.

[4] M. Mortazavi, "Turbulent Dispension and Diffusion: Phenomenological Theories and Stochastic Simulations", M-Sc Thesis, UCD, 1985.

List of Publications

[1] S. Byggstoyl, W. Kollmann: "Stress Transport in the Rotational and Irrotational Zones of Turbulent Shear Flows", Physics of Fluids 29 (1986), pp. 1423-1429.

[2] S. Byggstoyl, W. Kollmann, "A Closure Model for Conditional Stress Equations and Its Application to Turbulent Shear Flows", Physics of Fluids 29 (1986), pp. 1430-1440.

In Preparation

[3] M. Mortazavi, W. Kollmann: "The pdf Equation for Velocity and Vorticity and Its Application Conditional Closures".

[4] A. Wu, W. Kollmann: "Stochastic Simulation of the Velocity-pdf Equation for Parabolic Flows".

Professional Personnel

1. Arthur Wu, Ph.D. student, Department of Mechanical Engineering, graduated from California State University, Sacramento, 1983.

2. M. Mortazavi, Ph.D. student, graduated from the Department of Chemical Engineering, UC Davis, 1984.

3. W. Kollmann, Professor, Department of Mechanical Engineering, UC Davis, Principal Investigator.

Patents

No patents resulted from this research work.

Appendix I: Random walk simulation of scalar transport in turbulent flow.

M. Mortazavi's M.S. Thesis explored random walk Monte-Carlo simulation of turbulent dispersion. Both pair and single particle disperison were studied. Pair dispersion is intimately related to two point correlations.

Equations governing the position pdf and separation pdf of particles dispersed in an isotropic turbulence were derived by S. Goldstein (1951) and T. S. Lundgren (1981). S. Goldstein's equation is of the form:

$$\partial_{tt}^2 P + \frac{1}{A}\partial_t P = v^2 \partial_{xx}^2 P \qquad (1)$$

which contains both dissipative and non-dissipative terms. This p.d.e. was solved by Monte-Carlo technique and a sample solution with 100,000 particles appears in Figures (1A-E). The improvement in the numerical solution is marginal for particle numbers greater than 10^4.

Goldstein's equation [equation(1)] is valid for the idealized case of exponentially decaying Lagrangian velocity autocorrelation function. The generalization of the random walk to various Lagrangian velocity autocorrelation functions has been discussed in the thesis. As a simple example see Figure (2).

Monte-Carlo technique for solving equations of the form:

$$\partial_t P + \underline{\alpha} \cdot \underline{\nabla} P = \underline{\underline{K}} : \underline{\nabla}\,\underline{\nabla} P \qquad (2)$$

with constant $\underline{\alpha}$, dispersion tensor $\underline{\underline{\kappa}}$ (with positive eigenvalues) and arbitrary n-dimensional coordinate system was also developed. These type of equations occur in transport of scalars in porous media where P would be some spatially averaged scalar value.

Since we were concerned with the geometric characteristics of clusters of particles as they are translated, rotated and sheared by the turbulent field, it was natural to consider the equation which governs the separation probability of particles given the initial separation. The relevant equation was derived by Lundgren (1981) for isotropic turbulence. It is of the form:

$$\partial_t P_r = \underline{\nabla} \cdot (2\underline{\underline{D}} \cdot \underline{\nabla} P_r) \qquad (3)$$

Due to the dependence of $\underline{\underline{D}}$ on the phase space, Monte-Carlo simulation of this equation is extremely tedious. However, we applied the Monte-Carlo technique developed for solving equation (2) to equation (3). Some sample results are shown in Figures (3A,B) and (4). Experimental data in Figure (3A) were obtained by studying the separation of pairs of balloons released in the atmosphere by Julian (1977). While good numerical results were obtained for average separation (Fig. 3A) and root-mean-square of separation (Fig. 3B), poor results were obtained for the large time behaviour of cross correlations (Fig. 4). This is due to the approximate nature of the simulation. (The nature of the approximation is fully explained in the thesis.) Finally, we attempted to derive new random walk models that were higher order approximations to equation (3). The results of this line of investigation appears in the last chapter of the thesis. They have not been fully tested numerically.

References:

S. Goldstein, J. Mech. Appl. Math. 4, (1951), p. 129.

T. S. Lundgren, JFM 111 (1981), p. 27.

P. Julian et al., Bull. Am. Met. Soc. 5 (1977), p. 936.

FIGURES 1 A-E: N=100000, τ =d=0.005, p=0.9975, c=0.995

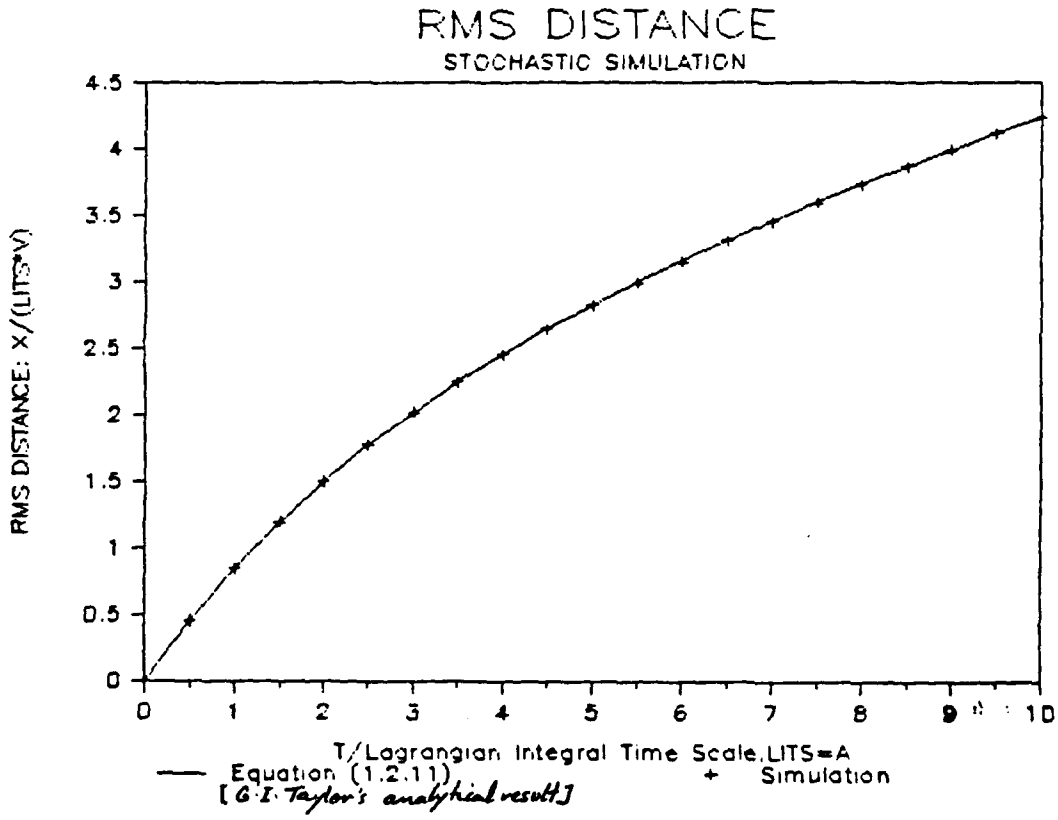

FIGURE 1 A RMS DISTANCE VS. TIME: COMPARISON OF STOCHASTIC SOLUTION WITH TAYLOR'S ANALYTICAL RESULT

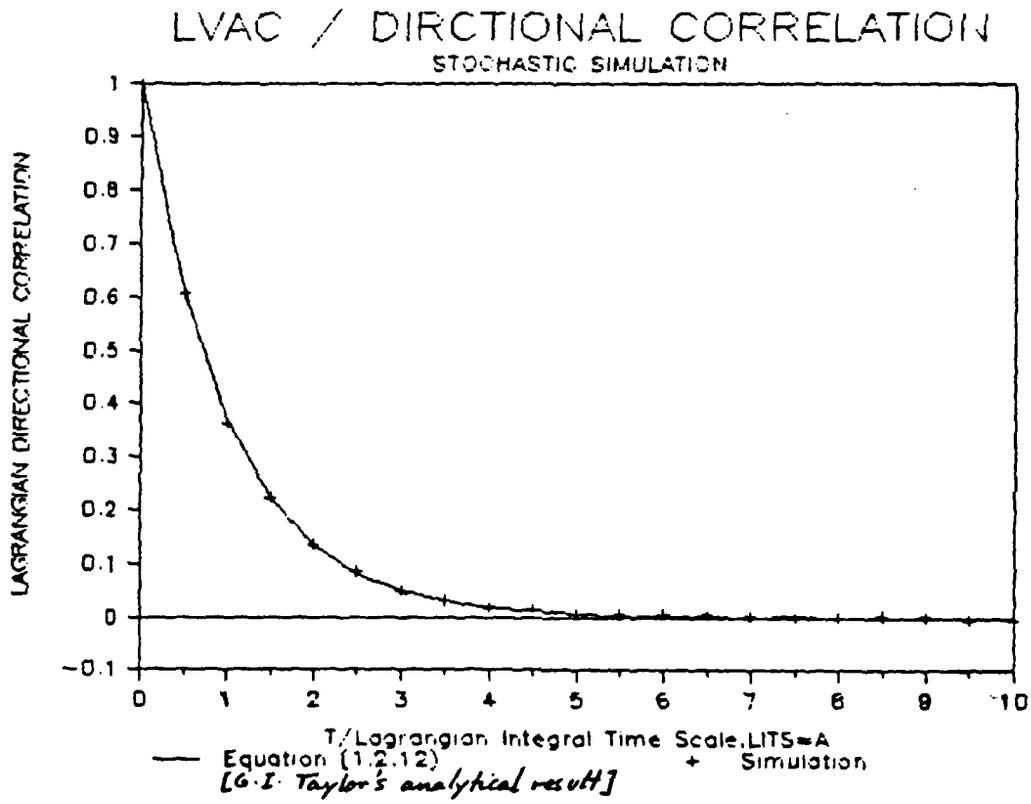

FIGURE 1 B LAGRANGIAN VELOCITY AUTOCORRELATION COEFFICIENT: COMPARISON OF STOCHASTIC SOLUTION WITH TAYLOR'S ANALYTICAL RESULT

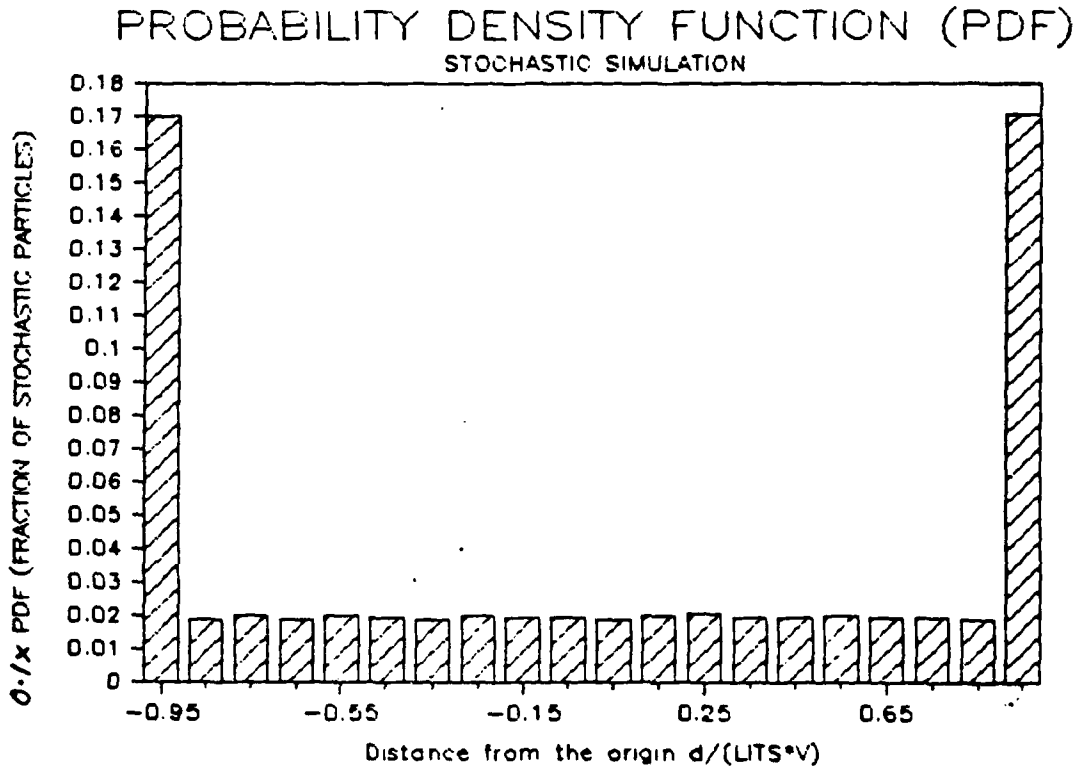

FIGURE 1 C PROBABILITY DENSITY FUNCTION OF PARTICLE POSITION AT T=A

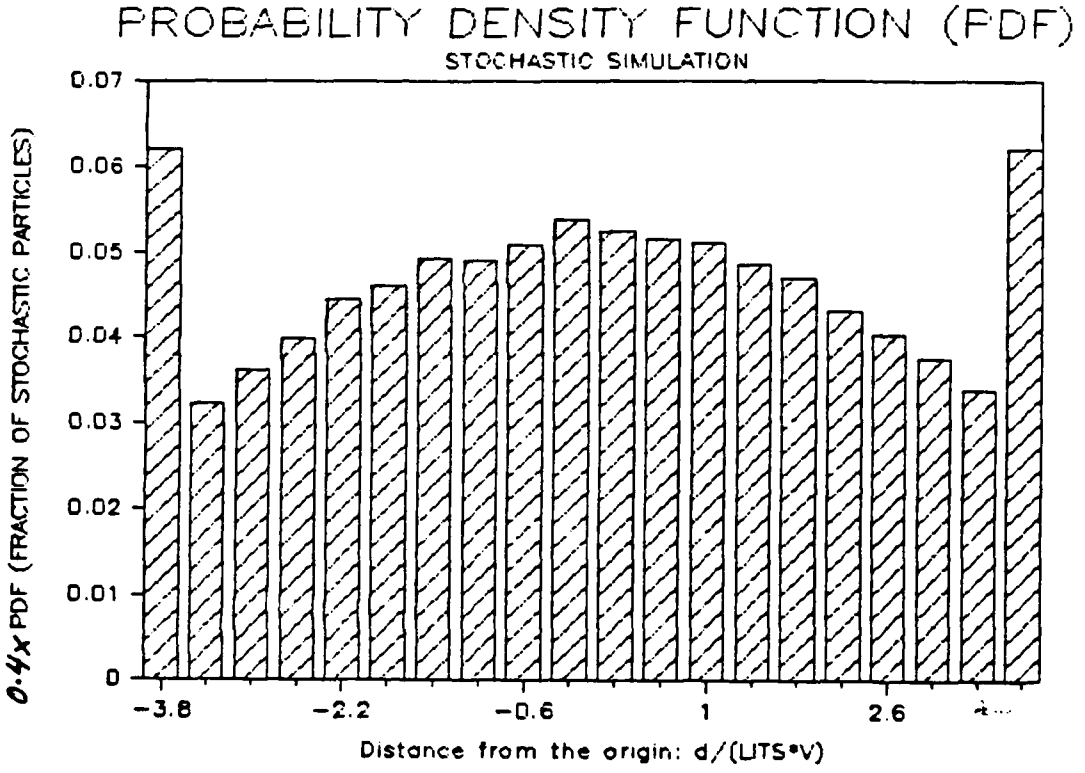

FIGURE 1 D PROBABILITY DENSITY FUNCTION OF PARTICLE POSITION AT T=4*A

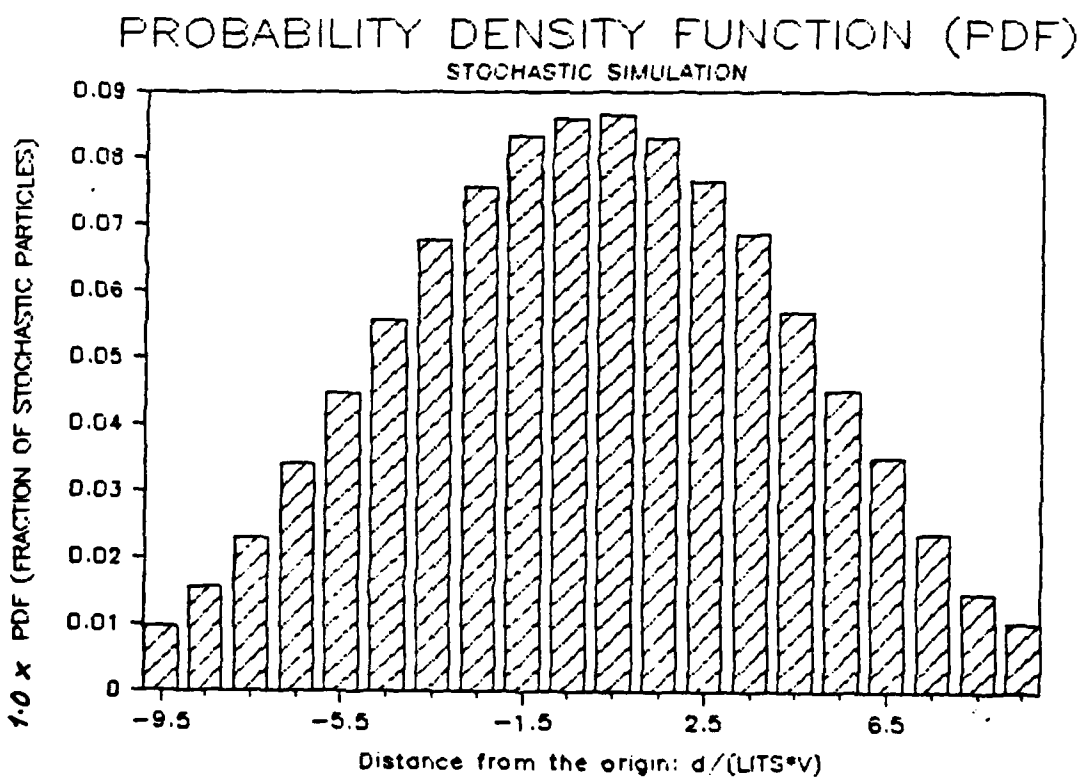

FIGURE 1 E PROBABILITY DENSITY FUNCTION OF PARTICLE POSITION AT T=10*A

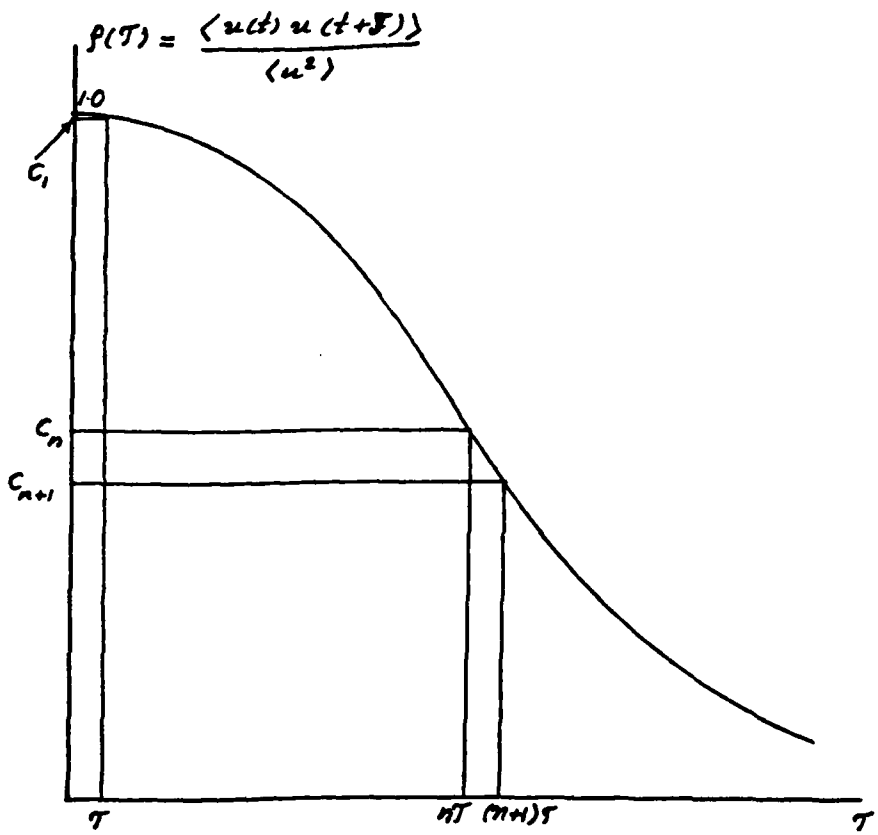

FIGURE 2 A GENERAL LVAC

The stochastic particle that had a velocity $+\bar{v}\hat{\imath}$ at the time interval $[0,\tau]$ will have possible velocities of $+\bar{v}\hat{\imath}$ and $-\bar{v}\hat{\imath}$ at the time interval $[n\tau, (n+1)\tau]$. The velocity of $+\bar{v}\hat{\imath}$ will occur with the probability $[(C_{n+1}+C_n)/2C_0+1]/2 = P_{n,0}$ and the velocity of $-\bar{v}\hat{\imath}$ will occur with the probability $1 - P_{n,0}$.

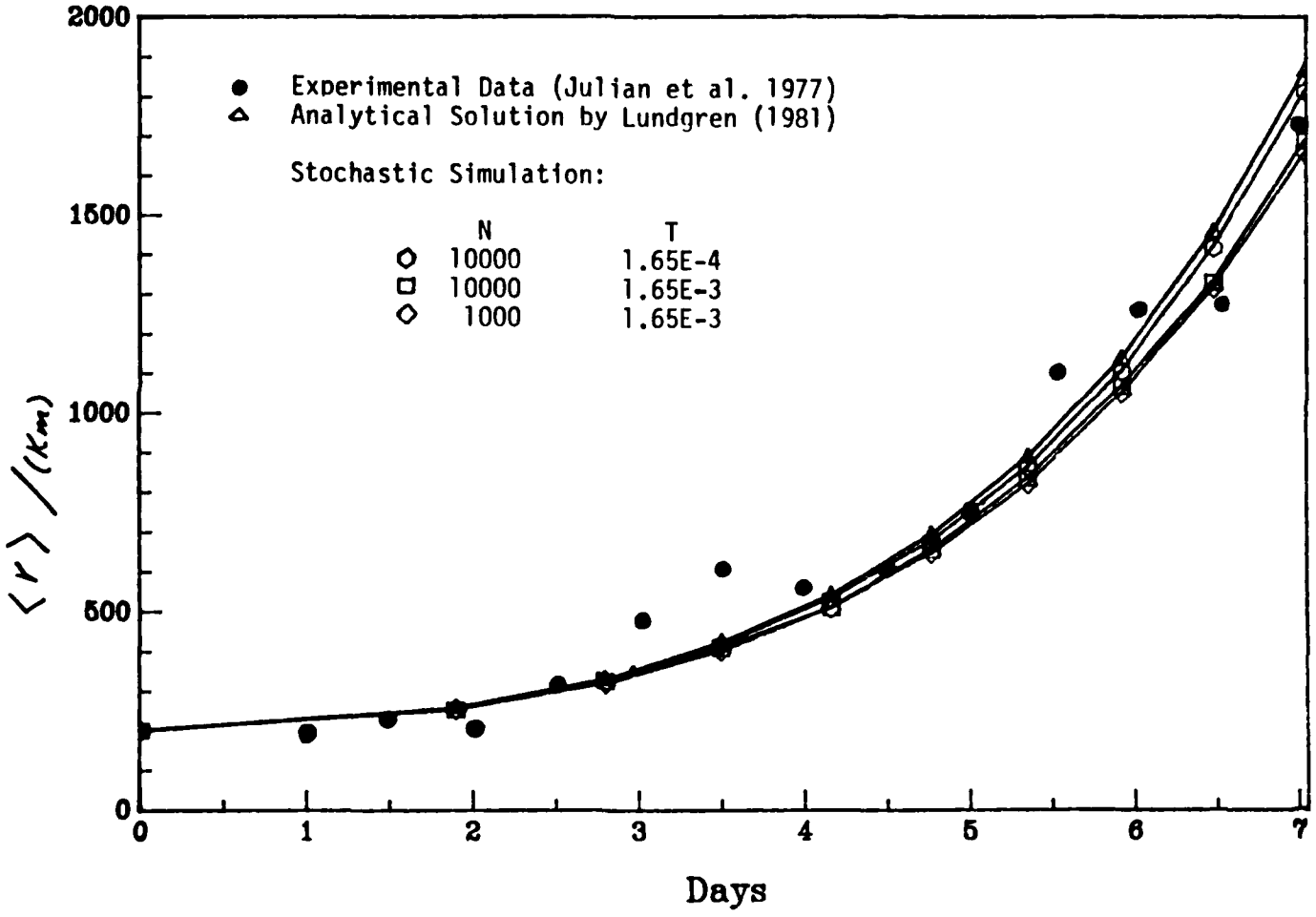

FIGURE 3(a) AVERAGE SEPARATION MAGNITUDE $\langle r \rangle$

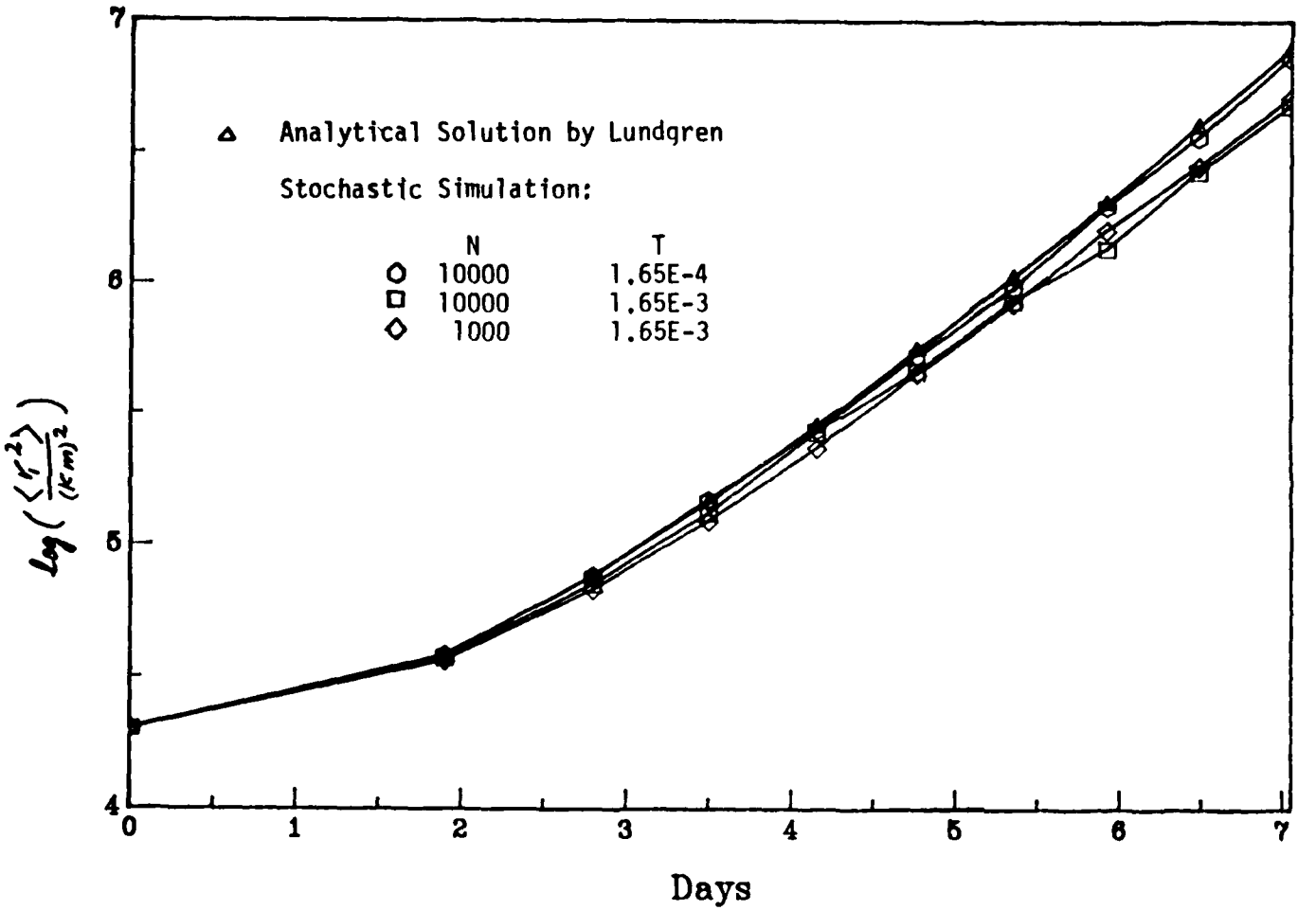

FIGURE 3(b) CORRELATION $\langle r^2 \rangle$

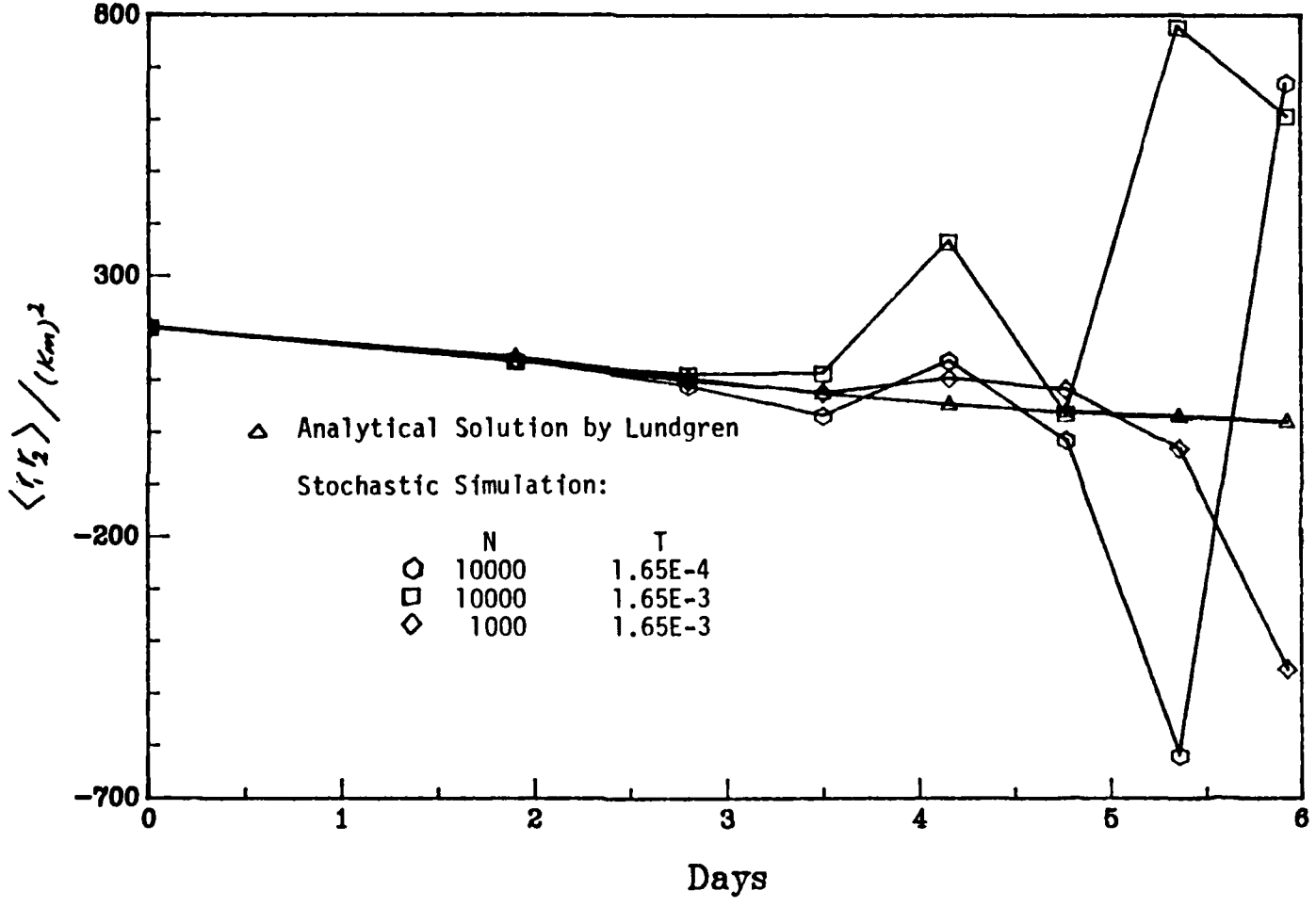

FIGURE 4 CROSS CORRELATION $\langle r_1 r_2 \rangle$

Appendix II: Comparison of diffusion closures for round jets (unconditioned case).

The transport equations for the Reynolds stress components $\langle u_\alpha' u_\beta' \rangle$ are given in the Cartesian frame by (constant density)

$$D_t \langle u_\alpha' u_\beta' \rangle = \partial_\gamma \left[\nu \partial_\gamma \langle u_\alpha' u_\beta' \rangle - \langle u_\alpha' u_\beta' u_\gamma' \rangle - \partial_{\beta\gamma} \frac{1}{\rho} \langle u_\alpha' p' \rangle - \right.$$

$$\left. - \partial_{\alpha\gamma} \frac{1}{\rho} \langle u_\beta' p' \rangle \right] - \langle u_\alpha' u_\gamma' \rangle \partial_\gamma \langle u_\beta \rangle - \langle u_\beta' u_\gamma' \rangle \partial_\gamma \langle u_\alpha \rangle$$

$$+ \frac{1}{\rho} \langle p' (\partial_\alpha u_\beta' + \partial_\beta u_\alpha') \rangle - \langle \varepsilon_{\alpha\beta} \rangle$$

where the rate of dissipation is defined by

$$\langle \varepsilon_{\alpha\beta} \rangle \equiv 2\nu \langle \partial_\gamma u_\alpha' \partial_\gamma u_\beta' \rangle$$

The closure of the stress transport equations follows established lines [1], [2]. The pressure-rate-of-strain correlation is split into "return to isotropy" and "fast response" parts.

$$\frac{1}{\rho} \langle p' (\partial_\alpha u_\beta' + \partial_\beta u_\alpha') \rangle \cong - C_1 \frac{\varepsilon}{k} \left(\langle u_\alpha' u_\beta' \rangle - \frac{2}{3} \partial_{\alpha\beta} k \right)$$

$$- \frac{C_2 + 8}{11} \left(P_{\alpha\beta} - \frac{2}{3} \partial_{\alpha\beta} P \right) - \frac{30 C_2 - 2}{55} k \left(\partial_\alpha \langle u_\beta \rangle + \partial_\beta \langle u_\alpha \rangle \right)$$

$$- \frac{8 C_2 - 2}{11} \left(D_{\alpha\beta} - \frac{2}{3} \partial_{\alpha\beta} P \right)$$

where

$$P_{\alpha\beta} \equiv - \langle u_\alpha u_\gamma' \rangle \partial_\gamma \langle u_\beta \rangle - \langle u_\beta' u_\gamma' \rangle \partial_\gamma \langle u_\alpha \rangle \quad , \quad P \equiv \frac{1}{2} P_{\alpha\alpha}$$

and

$$D_{\alpha\beta} \equiv - \langle u_\alpha u_\gamma' \rangle \partial_\beta \langle u_\gamma \rangle - \langle u_\beta u_\gamma' \rangle \partial_\alpha \langle u_\gamma \rangle$$

and $C_1 = 1.5$, $C_2 = 0.4$. The rate of dissipation is closed for high Re-numbers using the concept of local isotropy

$$\langle \varepsilon_{\alpha\beta} \rangle \cong \frac{2}{3} \partial_{\alpha\beta} \varepsilon$$

where $\mathcal{E} = \frac{1}{2}\langle \mathcal{E}_{\alpha\alpha} \rangle$ and the transport equation for ϵ is included in the closure model [1], [4]. For the diffusive flux of stress two closure models are considered.

(A) Daly-Harlow [5] model: This is a generalized gradient flux model given by

$$-\langle v_\alpha' v_\beta' v_\gamma' \rangle \cong C_s \frac{k}{\mathcal{E}} \langle v_\gamma' v_\delta' \rangle \partial_\delta \langle v_\alpha' v_\beta' \rangle$$

where $C_s = 0.22$.

(B) Lumley [2] model: This model is based on the condition that the statistics of the velocity fluctuations relax to Gaussian in the absence of non-homogeneities and driving forces. For the Cartesian frame it is given by

$$-\langle v_\alpha' v_\beta' v_\gamma' \rangle \cong$$

$$\cong C_I \frac{k}{\mathcal{E}} \left[F_{\alpha\beta\gamma} + C_{II} \left(\partial_\alpha F_{\beta\gamma} + \partial_\beta F_{\alpha\gamma} + \partial_\gamma F_{\alpha\beta} \right) \right]$$

where

$$F_{\alpha\beta\gamma} = \langle v_\delta' v_\gamma' \rangle \partial_\delta \langle v_\alpha' v_\beta' \rangle + \langle v_\beta' v_\delta' \rangle \partial_\delta \langle v_\alpha' v_\gamma' \rangle + \langle v_\alpha' v_\delta' \rangle \partial_\delta \langle v_\beta' v_\gamma' \rangle$$

and

$$F_\alpha = \langle v_\alpha' v_\delta' \rangle \partial_\delta k + \langle v_\gamma' v_\delta' \rangle \partial_\delta \langle v_\alpha' v_\gamma' \rangle$$

and

$$C_I = 0.15 \quad , \quad C_{II} = \frac{2 - 6\,C_I}{4 + 15\,C_I}$$

Note that the pressure fluxes $\langle u_k' p' \rangle$ are neglected.

For the tranformation to cylindrical coordinates the following definitions are introduced:

Cartesian		Cylindrical	
Coordinate	Velocity	Coordinate	Velocity
x_1	v_1	x	u
x_2	v_2	r	v_r
x_2	v_3	θ	v_θ

and

$$x = x_1 \qquad x_1 = x$$

$$r = \sqrt{x_2^2 + x_3^2} \qquad x_2 = r\cos\theta$$

$$\theta = \operatorname{arctg}\left(\frac{x_3}{x_2}\right) \qquad x_3 = r\sin\theta$$

In order to satisfy the symmetry conditions at the axis the following combinations of stresses are used as dependent variables [6]:

$$k \equiv \frac{1}{2}\left(\overline{u'^2} + \overline{v_r'^2} + \overline{v_\theta'^2}\right)$$

$$\overline{u'^2}$$

$$W \equiv \frac{1}{r^2}\left(\overline{v_\theta'^2} - \overline{v_r'^2}\right)$$

$$S \equiv \frac{1}{r}\,\overline{u'v'}$$

All variables must satisfy the zero-gradient condition at the axis and then the conditions

$$\overline{v_\theta'^2} = \overline{v_r'^2} \quad , \quad \overline{u'v'} = 0 \quad \text{for } r = 0$$

are fulfilled automatically.

The stress transport equations for boundary-layer-type flows without swirl for the variable combinations defined above are then given by:

$$\partial_t k + \langle u \rangle \partial_x k + \langle v_r \rangle \partial_r k =$$

$$= \frac{1}{r} \partial_r \left[r \left(\nu \partial_r k - \langle v_r' k' \rangle - \frac{1}{\rho} \langle p' v_r' \rangle \right) \right] - \langle u v_r' \rangle \partial_r \langle u \rangle - \varepsilon$$

$$\partial_t \langle u'^2 \rangle + \langle u \rangle \partial_x \langle u'^2 \rangle + \langle v_r \rangle \partial_r \langle u'^2 \rangle =$$

$$= -2 \langle u' v_r' \rangle \partial_r \langle u \rangle + \frac{1}{r} \partial_r \left[r \left(\nu \partial_r \langle u'^2 \rangle - \langle v_r' u'^2 \rangle - \frac{2}{\rho} \langle v_r' p' \rangle \right) \right]$$

$$+ \frac{2}{\rho} \left\langle p' \frac{1}{r} \partial_r (r v_r') \right\rangle - \langle \varepsilon_{xx} \rangle$$

$$\partial_t w + \langle u \rangle \partial_x w + \langle v_r \rangle \partial_r w =$$

$$= \frac{1}{r^3} \partial_r \left[r \left(\nu \partial_r \langle v_\theta'^2 \rangle - \langle v_r' v_\theta'^2 \rangle + \langle v_r'^3 \rangle + \frac{1}{\rho} \langle v_r' p' \rangle \right) \right]$$

$$- \frac{4}{r^3} \langle v_r' v_\theta'^2 \rangle + \frac{2}{\rho r^3} \langle p' (\partial_\theta v_\theta' - \partial_r (r v_r')) \rangle - \frac{1}{r^2} \left(\langle \varepsilon_{\theta\theta} \rangle - \langle \varepsilon_{rr} \rangle \right)$$

$$\partial_t S + \langle u \rangle \partial_x S + \langle v_r \rangle \partial_r S = \frac{1}{r^2} \partial_r \left[r \left(\nu \partial_r \langle u' v_r' \rangle - \langle u' v_r'^2 \rangle \right) \right]$$

$$- \frac{1}{r} \partial_r \langle u' p' \rangle + \frac{1}{r^2} \langle u' v_\theta'^2 \rangle - \frac{1}{r} \langle v_r'^2 \rangle \partial_r \langle u \rangle + \frac{1}{\rho} \left\langle p' \left(\partial_x v_r' + \frac{1}{r} \partial_\theta u' \right) \right\rangle$$

$$- \frac{1}{r} \langle \varepsilon_{xr} \rangle$$

The closure of the diffusion terms is given for models (A) and (B) as follows.

Model A (Daly-Harlow):

$$-\frac{1}{r}\partial_r\left(r\langle v_r' k'\rangle\right) \cong \frac{1}{r}\partial_r\left(r C_I \frac{k}{\varepsilon}\langle v_r'^2\rangle \partial_r k\right)$$

$$-\frac{1}{r}\partial_r\left(r\langle v_r' w'^2\rangle\right) \cong \frac{1}{r}\partial_r\left(r C_I \frac{k}{\varepsilon}\langle v_r'^2\rangle \partial_r\langle w'^2\rangle\right)$$

$$-\frac{1}{r^3}\partial_r\left[r\left(\langle v_r' v_\theta'^2\rangle - \langle v_r'^3\rangle\right)\right] - \frac{4}{r^3}\langle v_r' v_\theta'^2\rangle \cong$$

$$\cong \frac{1}{r}\partial_r\left(r C_I \frac{k}{\varepsilon}\langle v_r'^2\rangle \partial_r W\right) + 2 C_I \frac{1}{r}\frac{k}{\varepsilon}\langle v_r'^2\rangle \partial_r W$$

$$+ \frac{2}{r}\partial_r\left(C_I \frac{k}{\varepsilon}\langle v_r'^2\rangle W\right)$$

$$-\frac{1}{r^2}\partial_r\left(r\langle w' v_r'^2\rangle\right) + \frac{1}{r^2}\langle w' v_\theta'^2\rangle \cong$$

$$\cong \frac{1}{r^2}\partial_r\left(r^2 C_I \frac{k}{\varepsilon}\langle v_r'^2\rangle \partial_r S\right) + \frac{1}{r}\partial_r\left(C_I \frac{k}{\varepsilon}\langle v_r'^2\rangle S\right)$$

$$+ C_I \frac{k}{\varepsilon}\langle v_r'^2\rangle W$$

where $C_I = 0.22$ (same as for the Cartesian case).

Model B (Lumley):

$$-\frac{1}{r}\partial_r\left(r\langle v_r' k'\rangle\right) \cong \frac{1}{r}\partial_r\Big[r C_I \frac{k}{\varepsilon}\Big(2\langle v_r'^2\rangle \partial_r k - \frac{1}{2}\langle v_r'^2\rangle \partial_r\langle U^2\rangle - \frac{r^2}{2}\langle v_r'^2\rangle \partial_r W + r^2 S \partial_r S\Big)\Big] +$$

$$+ \frac{1}{r}\partial_r\Big[r^2 C_I \frac{k}{\varepsilon}\Big(S^2 - \big(\langle v_r'^2\rangle + \langle v_\theta'^2\rangle\big) W\Big)\Big]$$

$$-\frac{1}{r}\partial_r\left(r\langle v_r' U^2\rangle\right) \cong \frac{1}{r}\partial_r\Big\{r C_I \frac{k}{\varepsilon}\Big[\Big(1-\frac{1}{2}C_{II}\Big)\langle v_r'^2\rangle \partial_r\langle U^2\rangle$$

$$+ (2+C_{II}) r^2 S \partial_r S + 2 C_I \langle v_r'^2\rangle \partial_r k - \frac{1}{2} C_I r^2 \langle v_r'^2\rangle \partial_r W\Big]\Big\}$$

$$+ \frac{1}{r}\partial_r\Big\{r^2 C_I \frac{k}{\varepsilon}\Big[(2+C_I) S^2 - 2 C_I \langle v_r'^2\rangle W\Big]\Big\}$$

$$-\frac{1}{r^3}\partial_r\left[r\left(\langle v_r' v_\theta'^2\rangle - \langle v_r'^3\rangle\right)\right] - \frac{4}{r^3}\langle v_r' v_\theta'^2\rangle \cong$$

$$\cong \frac{1}{r}\partial_r\left\{r C_I \frac{k}{\varepsilon}\left[(2+C_{II})\langle v_r'^2\rangle \partial_r W - 2C_{II} S \partial_r S\right]\right\}$$

$$+ \frac{1}{r}\partial_r\left\{\frac{C_I}{r}\frac{k}{\varepsilon}\left[(1+C_{II})\langle v_r'^2\rangle \partial_r\langle U^2\rangle - (2+4C_{II})\langle v_r'^2\rangle \partial_r k\right]\right\}$$

$$+ \frac{2}{r}\partial_r\left\{C_I \frac{k}{\varepsilon}\left[\left((1+C_{II})\langle v_r'^2\rangle + C_{II}\langle v_\theta'^2\rangle - r^2 W\right)W - C_{II} S^2\right]\right\}$$

$$+ 6 C_I \frac{k}{\varepsilon}\langle v_r'^2\rangle \frac{1}{r}\partial_r W - 12 C_I \frac{k}{\varepsilon} W^2$$

$$-\frac{1}{r^2}\partial_r\left(r\langle U' v_r'^2\rangle\right) + \frac{1}{r^2}\langle U' v_\theta'^2\rangle \cong$$

$$\cong \frac{1}{r}\partial_r\left[r C_I \frac{k}{\varepsilon}\left[(2+C_{II})\langle v_r'^2\rangle \partial_r S + (1+C_{II}) S \partial_r k\right.\right.$$

$$\left.\left. + (C_{II} - \tfrac{1}{2}) S \partial_r\langle U^2\rangle - \tfrac{1}{2} r^2 S \partial_r W\right]\right\}$$

$$+ \frac{1}{r} C_I \frac{k}{\varepsilon}\left(2\langle v_r'^2\rangle \partial_r S - r^2 S \partial_r W\right) - 4 C_I \frac{k}{\varepsilon} S W$$

$$+ \frac{1}{r}\partial_r\left\{C_I \frac{k}{\varepsilon}\left[\left(2\langle v_r'^2\rangle + C_{II}\left(\langle v_r'^2\rangle + \langle v_\theta'^2\rangle\right) - r^2 W\right) S\right]\right\}$$

All other closure expressions follow immediately from the Cartesian case.

Both closure models (A) and (B) were applied to a round jet. The prediction of round jets requires one modification for the shear stress $(\overline{u'v'})$, where C_1 is increased to $C_1 = 2.5$. This is necessary to achieve the correct spreading rate for jets into stagnant surroundings. The jet considered was characterized by:

$\bar{U}_0 = 154 \frac{m}{s}$, $\bar{U}_e = 9.4 \frac{m}{s}$

$D = 0.00265\,m$

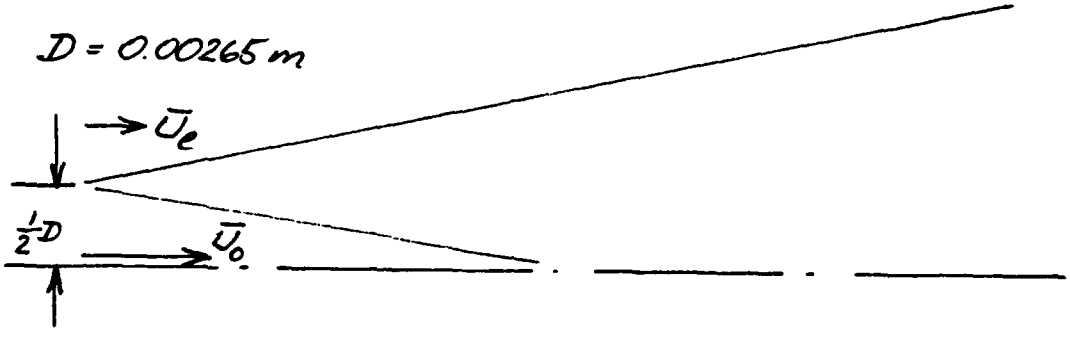

The results are presented in Fig. 1 to Fig. 7 for the station x/D = 70. The full line corresponds to case (A) and the broken line to case (B) except in Fig. 2, where all three normal stresses are plotted for case (A) and likewise Fig. 3 for case (B). The spreading rate

$$\frac{dy_{\frac{1}{2}}}{dx} \simeq 0.046$$

is virtually the same for both cases at this station. The main difference between (A) and (B) is the $(\overline{v'^2})$-profile which is larger in the outer front of the flow for case (B), which is Lumley's model, than for case (A), as can be seen from Figs. 2. 3. and 5. The shear stress in Fig. 7 is also larger for (B) than for (A) and consequently shows the mean velocity in Fig. 1 a longer tail for case (B).

Conclusions

The results show that Lumley's diffusion closure (B) has for axisymmetric flows the qualitatively the same features as for plane flows (see [4]). Recalling the properties of the nonturbulent zone fluctuations [3], where $\langle v'^2 \rangle$ becomes the dominant normal stress component, we conclude, that Lumley's diffusion closure should be superior to the gradient-flux-type model (A) for axisymmetric flows also.

References

[1] B. E. Launder, G J. Reece, and W. Rodi, JFM 68 (1975), pp. 537.

[2] J. L. Lumley, Adv. Appl. Mech. 18 (1978), pp. 123.

[3] S. Byggstoyl, W. Kollmann, Phys. Fluids 29 (1986), pp. 1423.

[4] S. Byggstoyl, W. Kollmann, Phys. Fluids 29 (1986), pp. 1430.

[5] B. J. Daly, F. H. Harlow, Phys. Fluids 13 (1970), pp. 2634.

[6] B. E. Launder, A. Morse, First Symp. Turb. Shear Flows, Penn. State Univ. (1977).

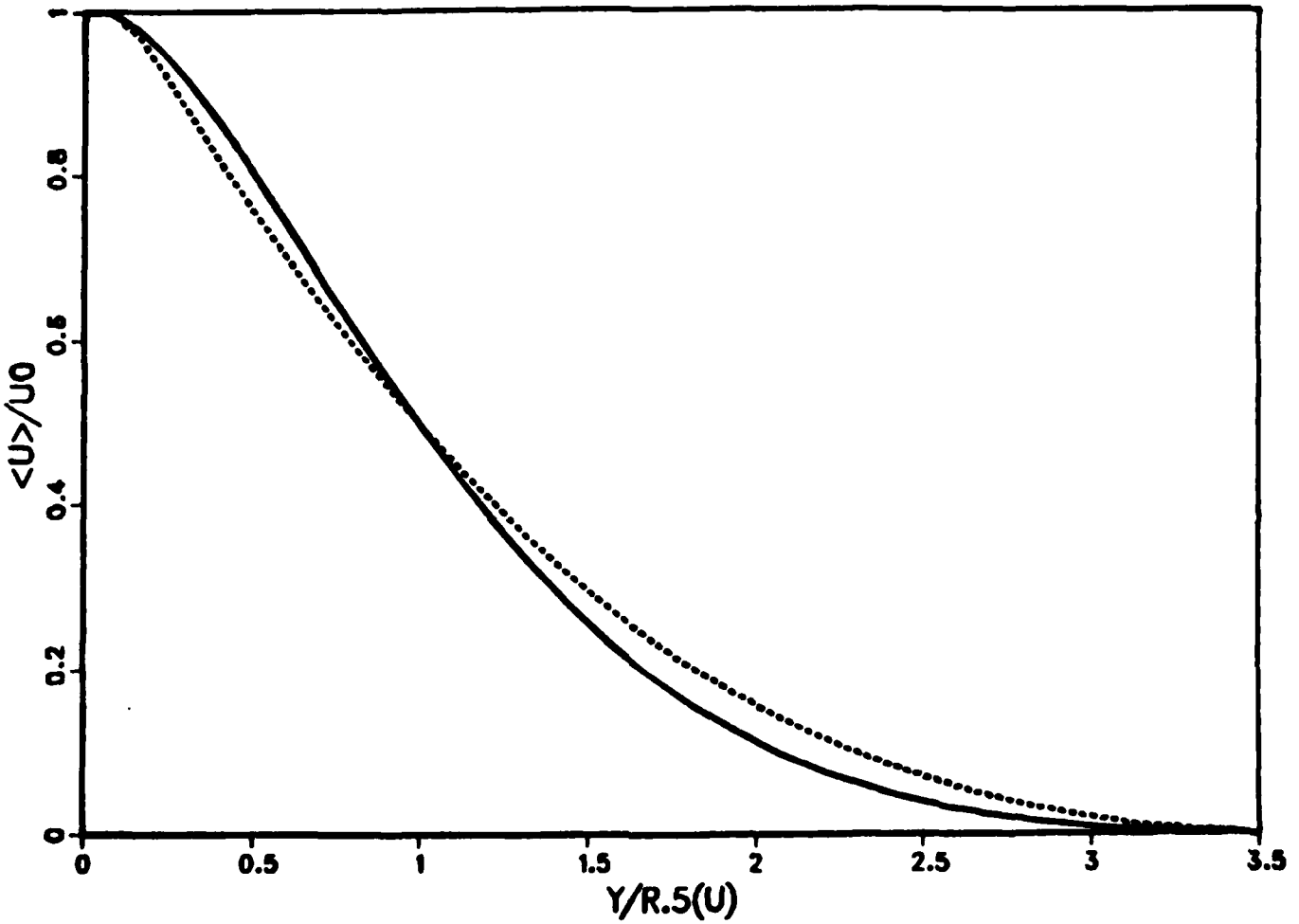

Fig. 1 Mean velocity $\frac{\langle U \rangle}{\langle U \rangle_{\ell}}$ at $\frac{x}{D}$ = 70.

Full line: case A, broken line: case B.

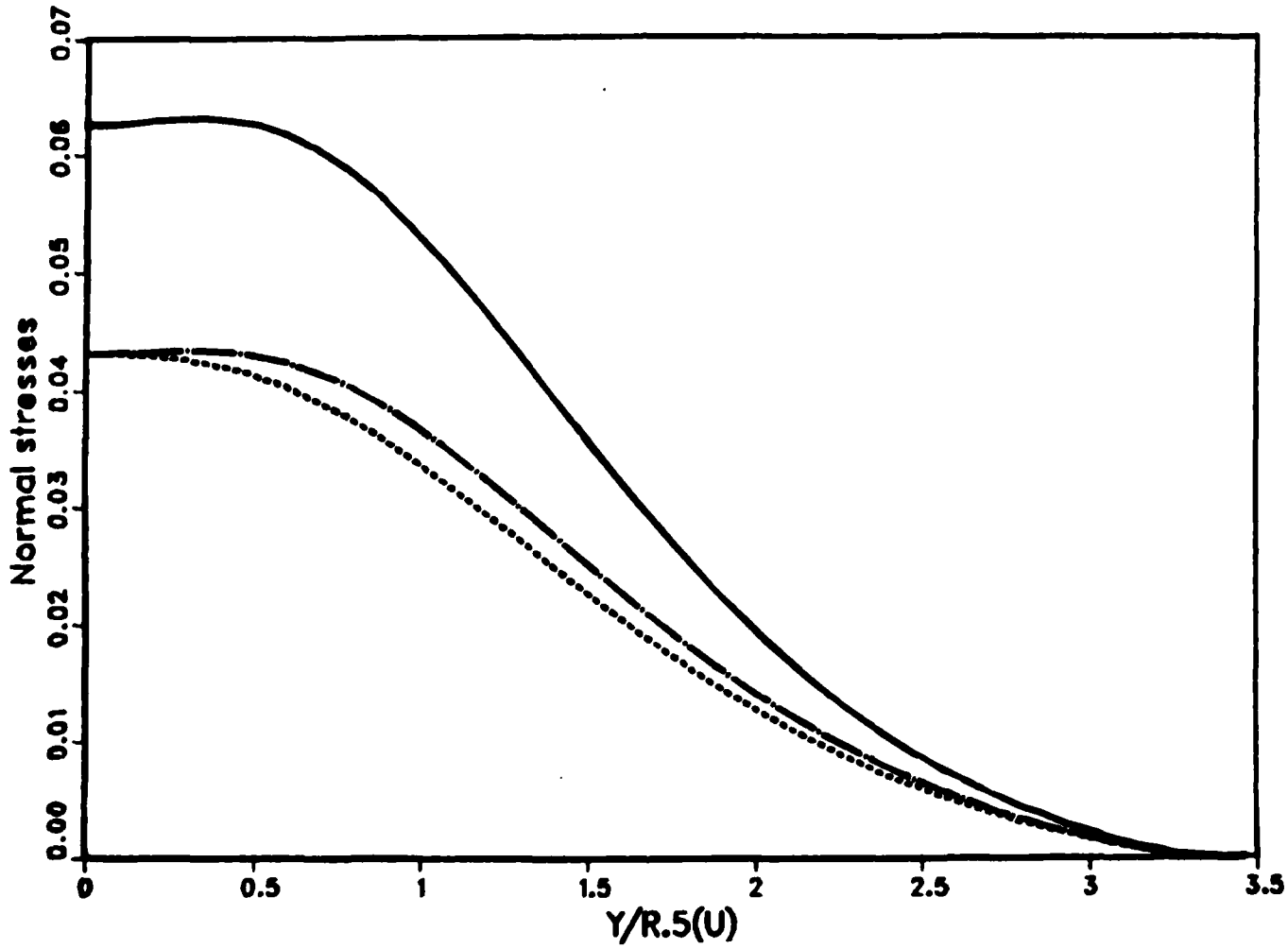

Fig. 2 Normal stresses at $\bar{S}$ = 70 for Case A.

Full line: $\langle u'^2 \rangle / \Delta U$, broken line: $\langle v'^2 \rangle / \Delta U$, dash dot line: $\langle w'^2 \rangle / \Delta U$

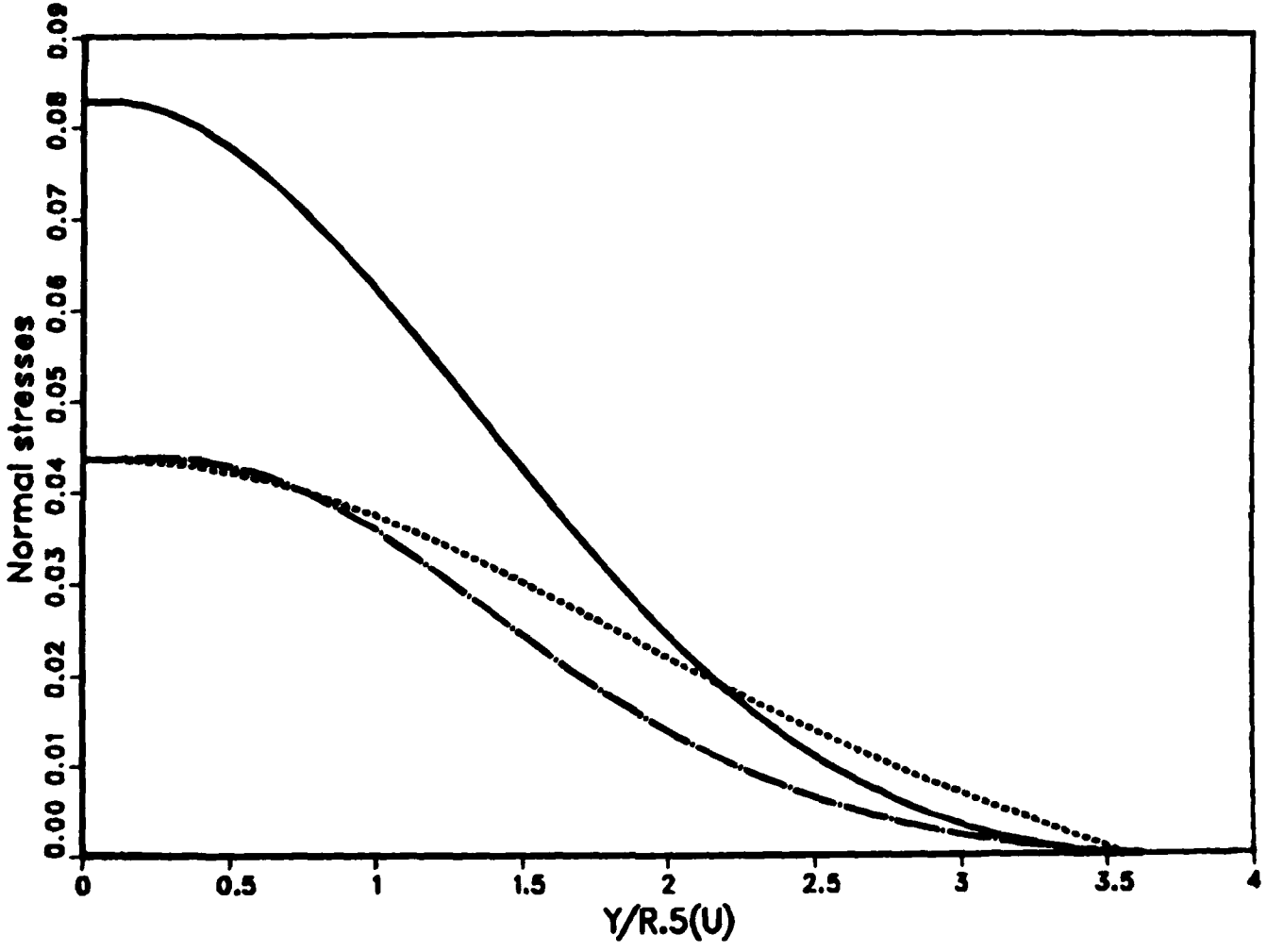

Fig. 3 Normal stresses at $\frac{x}{D}$ = 70 for case B.

Full line: $\langle u^2 \rangle / \Delta U$, broken line: $\langle v^2 \rangle / \Delta U$, dash dot line: $\langle v_\theta^2 \rangle / \Delta U$

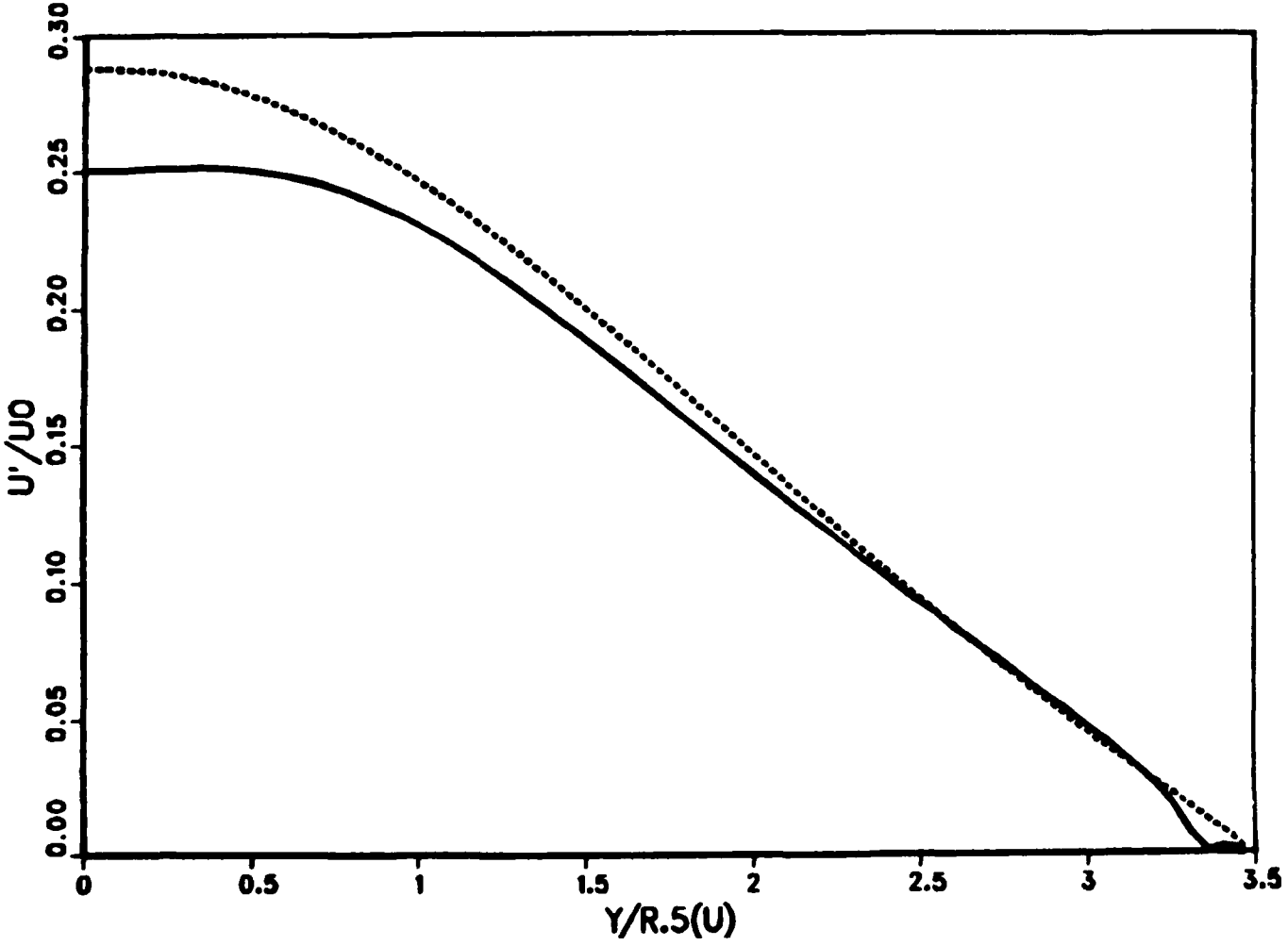

Fig. 4 Intensity $U'/\Delta U$ at $\frac{x}{D}$ = 70. Full line: case A, broken line: case B.

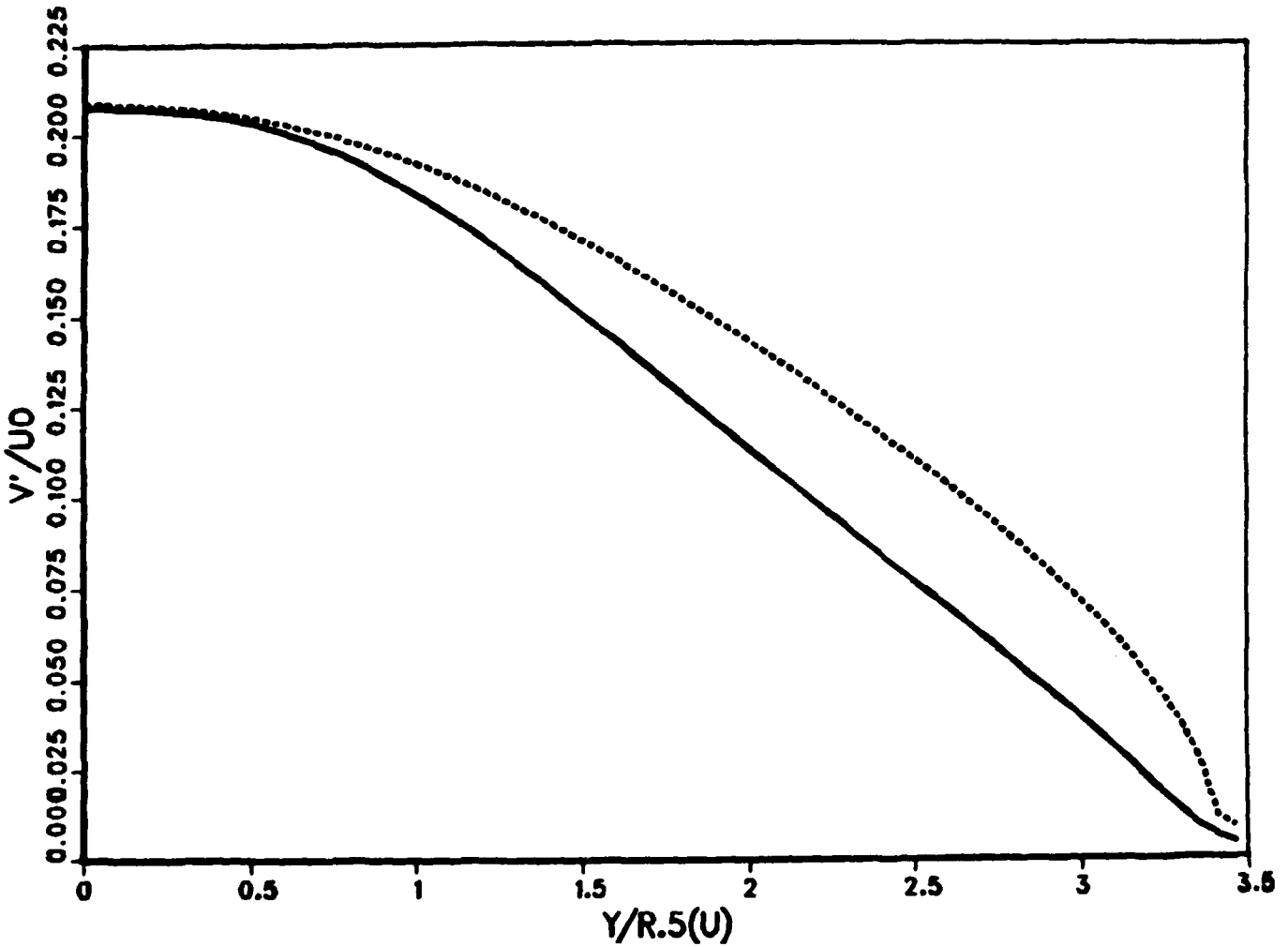

Fig. 5 Intensity $v'/\delta U$ at $\frac{x}{D}$ = 70. Full line: Case A, broken line: case B.

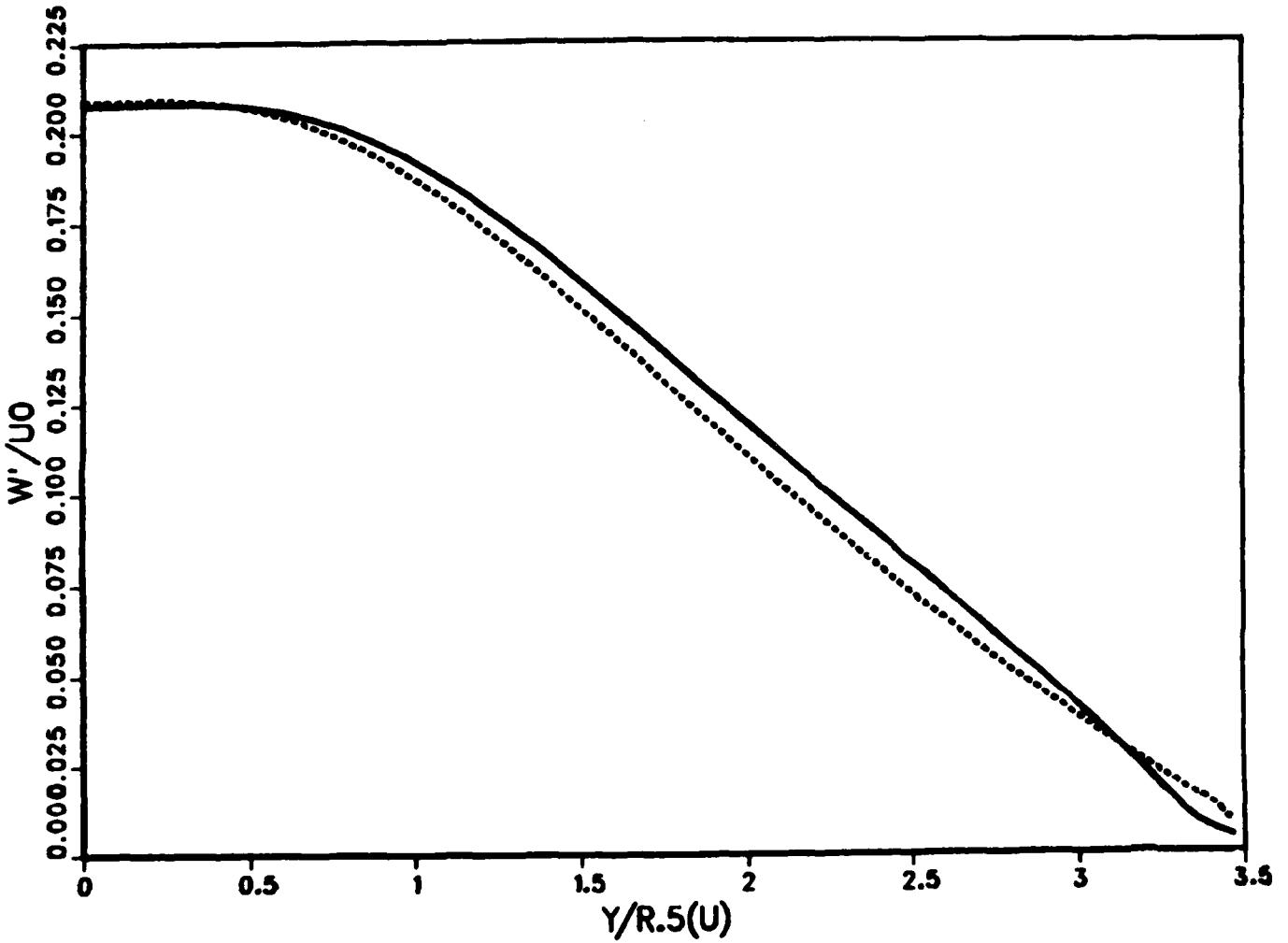

Fig. 6 Intensity $v'_o/\Delta U$ at $\frac{x}{D}$ = 70. Full line: case A, broken line: case B.

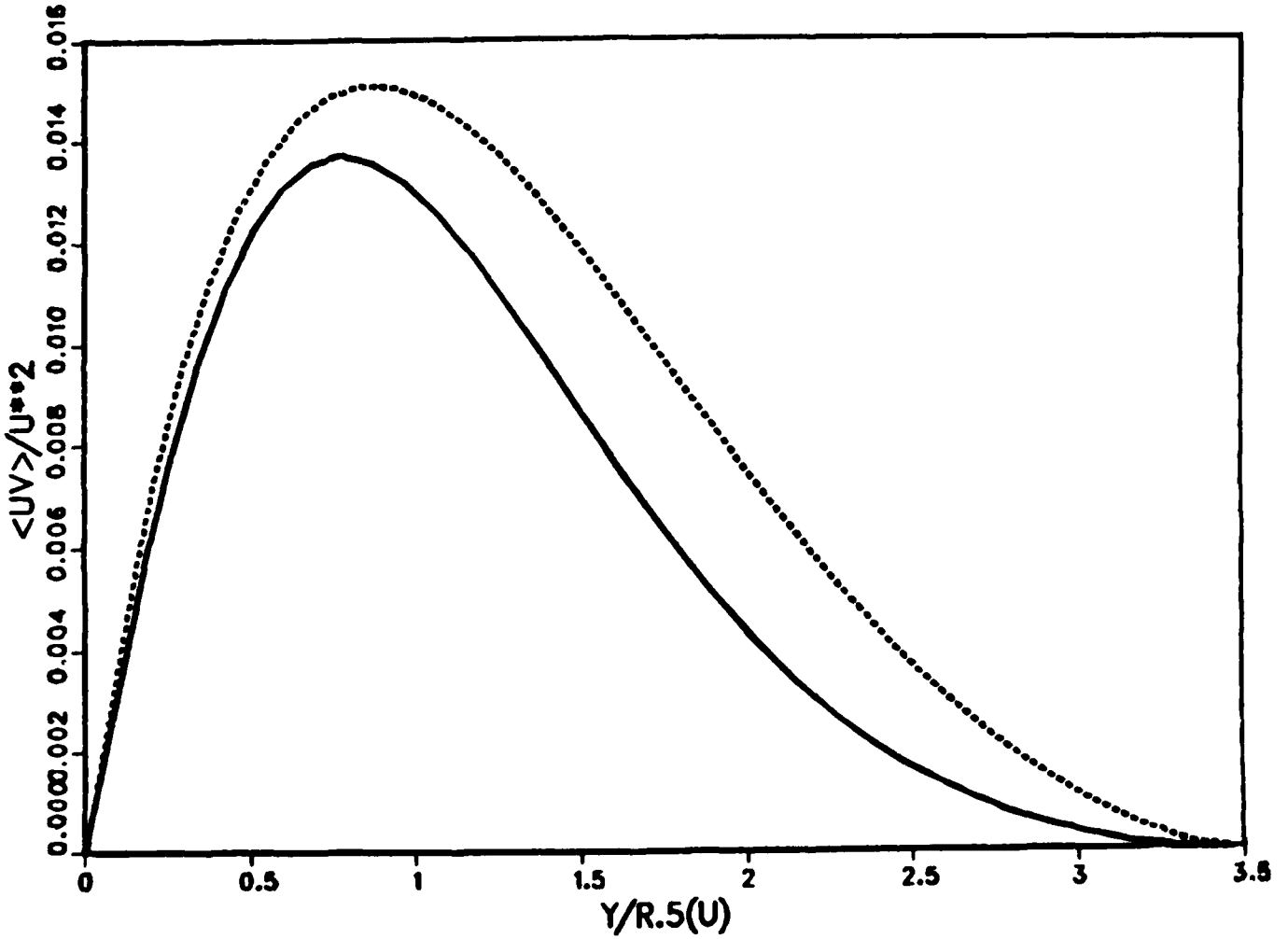

Fig. 7 Shear stress $\langle u'v' \rangle / \Delta U^2$ at $\frac{x}{D}$ = 70. Full line: case A, broken line: case B.

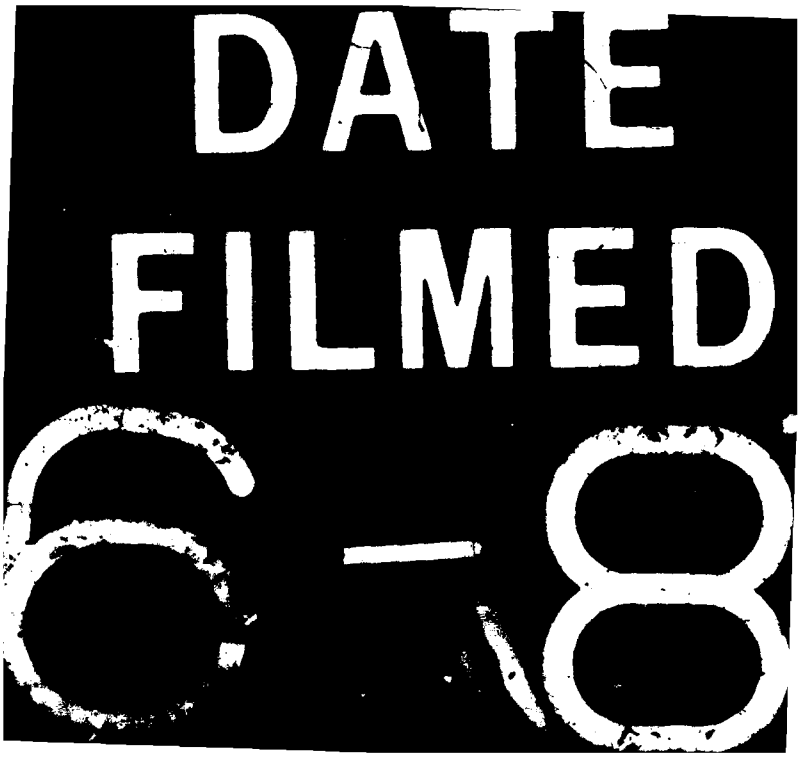
DATE
FILMED
6-8